

# Power fluctuations in the wavelet space: large-scale CMB non-gaussian statistics

L. Popa

*Institute for Space Sciences, Bucharest-Magurele, R-76900, Romania*

---

## Abstract

We analyse the large-scale coherence of the CMB anisotropy field with non-gaussian initial conditions using 2-point function of the power fluctuations in the wavelet space.

Employing the multivariate Edgeworth expansion (MEE) we constrain the normalization for the cosmic string mass-per-unit-length  $\mu$ , obtaining  $G\mu/c^2 = 1.075^{+0.455}_{-0.375} \times 10^{-6}$  at 68% CL in the standard gaussian statistics. This value is consistent with the results obtained from the simulations of the evolution of the string network and by other large scale studies.

*Key words:* Cosmology: cosmic microwave background, large scale structure -  
methodic: non-gaussian statistics, wavelet analysis

---

## 1 Introduction

The cosmic microwave background (CMB) provides one of the most useful tools for understanding the physical processes in the early universe, giving valuable information about the origin and the dynamics of the primordial fluctuations that seeded the today large-scale structures. There are two competing families of cosmological theories quite distinct in this regards.

In the models invoking most types of inflation [1–3] the perturbations' generation mechanism is linear and gaussian fluctuations are predicted. For a given type of inhomogeneity (adiabatic or isocurvature) the only degree of freedom in the initial conditions is the amplitude, and since the evolution is linear, solutions scale linearly with the initial amplitude. Linearity combined with the assumed statistical homogeneity of the universe guarantees that one may decompose the cosmological perturbations into eigenmodes with eigenfunctions that evolve independently. In the Fourier space, for instance, the evolution of a perturbation in each mode  $k$  is independent. For a finite sample of the CMB field, the observed fluctuations are the convolution of the “true” fluctuations

of the infinite field with the Fourier transform of a mask [13]. The 2-point function of the the power fluctuations depends only on the selection function [13,14].

The second class of theories, most topological defect models [4–6] and some versions of inflation [7], predict non-gaussian statistics of the primordial perturbations. Those models involve spontaneous symmetry breaking as the hot early universe cooled leading to a non-linear perturbations' generation mechanism. For this type of perturbations the Fourier modes  $k$  are coupled and their evolution cannot be anticipated on the basis of the initial conditions [8,10]. The predicted angular power spectrum has a position dependence with a variance larger than the variance of the angular power spectrum for the gaussian case at the same multipole order [9,10]. The defect theories are highly constrained by causality, the fluctuations being completely uncorrelated beyond the horizon scale at all times [8,11].

It is difficult to make difference between gaussian and non-gaussian fluctuations of the density field at large angular scales because of the tendency of any distribution to approach gaussian statistics when averaging over large area (the central limit theorem), and also because of the cosmic and sampling variances.

In this paper we propose the wavelet transform to analyse the large scale coherence of the CMB anisotropy field with non-gaussian initial conditions. The main advantage of the wavelet transform over the Fourier transform is its capability to investigate features of the CMB anisotropy maps with a resolution according to their scales [15]. The wavelet base functions are highly localized in space and the information regarding the scale and the position are stored explicitly. Also, the wavelet analysis can be performed with a finite sample of data in contrast with the Fourier analysis where the result depends on the selection function.

We employ 2-point function of power fluctuations in the wavelet space to compare COBE-*DMR* 4-year temperature anisotropy maps to the predictions of an analytical cosmic string model [21]. The advantage of the analytical approach is that one can obtain statistical fluctuations with non-gaussian random phases for a given experimental configuration, while the explicit dependences on the normalization of the primordial power spectrum, string parameters and angular scales can be shown.

We use the non-gaussian likelihood function to constrain the dimensionless cosmic string parameter  $G\mu/c^2$  (where  $G$  is the Newton's constant,  $c$  is the speed of light and  $\mu$  the the mass per unit length of the cosmic strings) at 68% CL in standard gaussian statistics, by comparing zero lag autocorrelation function from COBE-*DMR* with the predictions of the cosmic string model.

## 2 Monte-Carlo simulations

According to the scaling solution for cosmic strings [17,18] there is a fixed number  $M$  of strings with the curvature radius of the order of the horizon per Hubble volume at any given time, with orientations and velocities uncorrelated over distances larger than the horizon. The temperature anisotropy induced by long strings is given by Kaiser-Stebbins formula [19]:

$$\frac{\delta T}{T} = \pm 4\pi G\mu |\hat{k} \cdot (\gamma_s v_s \times \hat{e}_s)|,$$

where:  $\hat{k}$  is the direction of observation,  $v_s$  is the velocity of the string with the orientation  $\hat{e}_s$ ,  $\gamma_s = (1 - v_s/c)^{1/2}$ ,  $G$  is the Newton's constant and  $\mu$  is the mass per unit length of the string.

The time from the last scattering surface until now is divided into  $N$  Hubble time steps  $t_i$  with  $t_{i+1} = 2t_i$  and  $N = \log_2(t_0/t_{ls})$ . The apparent angular size of a Hubble volume at time  $t_i$  is  $\theta_{H_i} \sim z_i^{-1/2} \sim t_i^{1/3}$  and  $\theta_{H_{i+1}} = 2^{1/3}\theta_{H_i}$  for large redshifts in the matter dominated era assuming  $\Omega_0 = 1$ .

For an experiment measuring a square map of size  $\theta^0 \times \theta^0$  at each Hubble time  $t_i$  the number of  $n_i$  string segments random placed over the area size  $(\theta^0 + \theta_{H_i})^2$  is given by [20]:

$$n_i = M(\theta^0 + \theta_{H_i})^2 / \theta_{H_i}^2. \quad (1)$$

We use an analytical statistical string model [21] to take into account the combined effects of the temperature fluctuations induced by strings present between the redshift  $z \simeq 250$  and today ( $N = 12$ ).

We calculate the probability distribution functions of the temperature fluctuations induced by cosmic strings for different values of the string scaling solution parameter  $M$  by Fourier transforming the characteristic function of this model normalized to approach a gaussian distribution with zero mean and  $\sigma = 1$  when  $M \rightarrow \infty$  [21].

We generated CMB independent realizations, each of 6144 pixels, using the spherical harmonic representation:

$$\frac{\delta T}{T}(\theta, \phi) = \sum_{l=2}^{30} \sum_{m=0}^l a_{lm} W_l Y_{lm}(\theta, \phi). \quad (2)$$

where  $W_l$  is the DMR gaussian window function with FWHM=7°.

The harmonic coefficients  $a_{lm}$  are random variables with zero mean and the variances given by [22]:

$$\langle a_{lm}^2 \rangle = Q_{rms-PS}^2 \frac{4\pi}{5} \frac{\Gamma[l + (n-1)/2] \Gamma[(9-n)/2]}{\Gamma[l + (5-n)/2] \Gamma[(3+n)/2]}, \quad (3)$$

where:  $Q_{rms-PS}$  is the quadrupole normalized amplitude and  $n$  is the spectral index of the primordial power spectrum.

The coefficients  $a_{lm}$  are drawn from parent populations obtained in the cosmic string model. The non-gaussian amplitude distributions of  $a_{lm}$  with random phases convoluted with the spherical harmonics  $Y_{lm}(\theta, \phi)$  are characterized by a positive kurtosis in the resulting temperature distribution.

We generated 800  $n = 1$  full-sky realizations for each model defined by  $Q_{rms-PS}$  and  $M$ . To each realization we added a realization of the noise determined by the instrument sensitivity and the number of observations per pixel of DMR 4-year 53GHz (A+B)/2 map, and rejected the pixels with galactic latitude  $-19^\circ < b < 20^\circ$  obtaining  $2^{12}$  pixels.

We generated also in the same conditions 800  $n = 1$  full sky realizations for the same values of  $Q_{rms-PS}$  with  $a_{lm}$  drawn from a standard gaussian distribution with zero mean and  $\sigma = 1$ .

### 3 Two point function of power fluctuations in the wavelet space

A wavelet [15]  $\Psi(x) \in R$  is a function whose binary dilatation and dyadic translations generate an orthonormal base so that any function  $f(x) \in R$  can be approximated up to an arbitrarily small precision by:

$$f(x) = \sum_{i \in N} \sum_{j=0}^{2^i-1} c_j^i \Psi(2^i x - j). \quad (4)$$

The base functions  $\Psi(x)$  are labeled by the scale  $i$  and the position  $j$  ( $i, j \in N$ ). The wavelet coefficients  $c_j^i$  are real quantities containing all the information as that contained by the Fourier coefficients. The major difference is the number of indices, that is, in wavelet analysis the scale  $i$  and the position  $j$  in the scale are explicitly stored. The wavelet base functions  $\Psi(x)$  satisfy the scaling equation:

$$\Psi_j^i(x) = 2^{-i/2} \Psi(2^{-i}(j - x)). \quad (5)$$

Let  $V_{H_i}$  be the Hubble volume spanned by the scaling function  $[\Phi(2^i x - j)]_{j \in N}$  at the scale  $i$ . From the scaling equation it follows that:

$$\dots \subset V_{H_{i-1}} \subset V_{H_i} \subset V_{H_{i+1}} \subset \dots$$

This hierarchical structure ensures the multi-resolution capability of the wavelet analysis.

The orthogonality condition:

$$\langle \Psi_j^i \Psi_{j'}^{i'} \rangle = \frac{1}{2^i} \delta_{j,j'} \delta_{i,i'}, \quad (6)$$

yields to:

$$c_j^i = 2^i \sum_k f(x_k) \Psi_j^i(x_k). \quad (7)$$

This last equation represents our wavelet transform convention.

For a random gaussian field the ensemble-averaged power  $\hat{P}(\Delta\theta)$  in the wavelet space at the separation angle  $\Delta\theta$  is:

$$\langle c_j^i(\vec{n}_1) c_{j'}^{i'}(\vec{n}_2) \rangle_{\Delta\theta} = \delta_{i,i'} \delta_{j,j'} \hat{P}(\Delta\theta), \quad (8)$$

where  $\vec{n}_1$  and  $\vec{n}_2$  are two directions in the sky separated by  $\Delta\theta$ .

For a random non-gaussian field generated using the cosmic string model the intrinsic correlations exist only within the same scale and the equation (8) becomes:

$$\langle c_j^i(\vec{n}_1) c_{j'}^{i'}(\vec{n}_2) \rangle_{\Delta\theta} = \delta_{i,i'} \hat{P}_{jj'}(\Delta\theta), \quad (9)$$

and  $\hat{P}_{jj'}(\Delta\theta)$  contains the correlated ensemble-averaged signal.

We define the 2-point function of the power fluctuations in the wavelet space as:

$$\xi_P(\Delta\theta) = \delta \hat{P}_{jj'}(\Delta\theta) = \hat{P}_{jj'}(\vec{n}_1) \hat{P}_{jj'}(\vec{n}_2) - \hat{P}_{jj'}(\Delta\theta). \quad (10)$$

In this paper we present the results obtained using Daubechies wavelet base functions of order 4 as a typical compact orthonormal base.

The wavelet transform applied on 2D map (with  $2^{12}$  pixels and  $i = 12$  uncorrelated scales) acts in a pyramidal algorithm, stripping the initial map scale by scale into its correlated components. The reader may refer to the references [16,23] for complete information.

Figure 1 presents the distributions of spots as a function of threshold (expressed in number of standard deviations) obtained for the averaged simulated maps in real and wavelet space for two types of simulations:  $a_{lm}$  with random gaussian phases (panels a and b), and  $a_{lm}$  with random non-gaussian phases, obtained in the cosmic string model with  $M = 10$  (panels c and d). For all simulations we take  $Q_{rms-PS} = 18\mu\text{K}$ . In each case the gaussian fits are also shown. One can see that the differences between the distributions obtained in gaussian and non-gaussian case are more evident in the wavelet space than in

the real space.

The maps obtained by Monte-Carlo simulations were wavelet transformed and then 2-point functions of the power fluctuations were constructed (binned in  $n = 36$  bins, in the manner of COBE-DMR).

Figure 2 presents the 2-point function of the power fluctuations in the wavelet space  $\xi_P(\Delta\theta)$  normalized at  $\xi_P(0)$ . The solid curve represents the theoretical prediction if the underlying distribution is gaussian and  $Q_{rms-PS} = 18\mu\text{K}$ . The error bars are based on Monte-Carlo simulations in the cosmic string model with  $M = 10$  and the same normalization.

#### 4 Non-Gaussian Likelihood analysis

According to the standard  $\chi^2$  method, if a specific model defined by the parameters  $(Q_{rms-PS}, M)$  is more likely to have occurred higher is the probability to obtain values of the  $\chi^2$  larger than the measured  $\chi_0^2$ . The cumulative probability used to define the confidence regions on the parameters is given by the integral:

$$I(\chi_0^2) = \int_0^{\chi_0^2} L(\lambda, \chi^2) d\chi^2, \quad (11)$$

where  $L$  is the likelihood function full specified by the  $\chi^2$  value and the covariance matrix. We define the  $\chi^2$  as:

$$\chi^2 = \sum_{i=1}^{36} \sum_{j=1}^{36} (\langle \xi_P^i \rangle - \xi_P^{DMR}) \lambda_{ij}^{-1} (\langle \xi_P^j \rangle - \xi_P^{DMR}). \quad (12)$$

where  $\langle \xi_P \rangle$  is the ensemble-averaged value of the 2-point function of the power fluctuations for Monte-Carlo realizations and  $\xi_P^{DMR}$  is the two point function of the power fluctuations for DMR data.

The covariance matrix  $\lambda_{ij}$  calculated for the the Monte-Carlo realizations is:

$$\lambda_{ij} = \frac{1}{N_{realiz}} \sum_{k=1}^{N_{realiz}} (\xi_P^k - \langle \xi_P \rangle) (\xi_P^k - \langle \xi_P \rangle). \quad (13)$$

The standard Gaussian likelihood statistic  $L_g$  associated to the two point function of the power fluctuation  $\xi_P(\Delta\theta)$  is given by:

$$L_g = \frac{e^{-\frac{1}{2}\chi^2}}{(2\pi)^{n/2} (\det\lambda)^{1/2}}. \quad (14)$$

In the case of non-gaussian random fields the confidence regions of the parameters depend also on the higher order correlation functions. It is shown that for mild non-gaussianity the likelihood function can be obtained within the multivariate Edgeworth expansion (MEE) [12]. According to MEE the total likelihood function is:

$$L = L_g + L_{ng}, \quad (15)$$

where  $L_{ng}$  is the non-gaussian correction which embodies the higher order moments of the data.

The integral in equation (11) can be written as:

$$I(\chi_0^2) = F_n(\chi_0^2) + Q_n(\chi_0^2), \quad (16)$$

where  $F_n(\chi_0^2)$  is the integral of gaussian likelihood, that is the cumulative integral of the  $\chi^2$  probability distribution with  $n = 36$  degrees of freedom, and  $Q_n(\chi_0^2)$  is a non-gaussian correction that depends on the higher order moments.

For each set of Monte-Carlo simulations we estimated the cumulative probability  $I(\chi^2)$ .

Figure 3 presents  $I(\chi^2)$  obtained for the models with  $Q_{rms-PS} = 18\mu K$  and few values of the  $M$  parameter compared with the same probability obtained for the gaussian case (the upper curve).

One can see that for mild non-gaussian fields the confidence regions are larger than the confidence regions in the gaussian case at the same  $\chi^2$  threshold.

Using the gaussian likelihood given by equation (14) we found  $Q_{rms-PS} = 18.29 \pm 1.36\mu K$  when the DMR 53GHz (A+B)/2 map was compared with the Monte-Carlo simulations obtained for a gaussian underlying distribution.

Figure 4 presents the confidence regions obtained for the parameters  $Q_{rms-PS}$  and  $M$  in cosmic string models at  $\chi_0^2 = 31.1$  that corresponds to 68% CL for a purely gaussian statistics.

Considering the region with  $I(\chi_0) \geq 0.3$  and taking the extrema of this contour we found that DMR data favorize the cosmic string models with  $M$  within 10 and 12 and  $Q_{rms-PS}$  within  $17.76\mu K$  and  $20.24\mu K$  at 68% CL for the standard gaussian statistics. We estimated the dimensionless cosmic parameter  $G\mu/c^2$  by comparing, in the wavelet space, the averaged zero lag autocorrelation function obtained in those models with zero lag autocorrelation function of DMR 4-year 53GHz (A + B)/2 map. We found:

$$G\mu/c^2 = 1.075_{-0.375}^{+0.455} \times 10^{-6}. \quad (17)$$

There are two terms that contribute to the error: a symmetrical error ( $\pm 0.185$ ) originating from the width of the confidence region and an asymmetric error given by the cosmic and sampling variances.

## 5 Conclusions

In this paper we propose the wavelet analysis for studying the large-scale CMB correlations induced by the cosmic strings.

Using an analytical cosmic string model to generate CMB temperature fluctuations with non-gaussian random phases in the COBE-*DMR* experimental configuration, and 2-point function of the power fluctuations in the wavelet space, we constrain the normalization of the primordial power spectrum  $Q_{rms-PS}$  and the parameter of the cosmic string scaling solution  $M$ .

We found that the large-scale CMB anisotropy favourizes the cosmic string models with large number of strings per Hubble volume,  $M=10, 11$  and  $12$  and  $Q_{rms-PS}$  from  $17.76\mu\text{K}$  to  $20.24\mu\text{K}$  at 68% CL for the standard gaussian statistics.

By comparing zero lag autocorrelation function of COBE-*DMR* 53GHz (A+B)/2 map with our predictions we obtained the dimensionless cosmic string parameter  $G\mu/c^2 = 1.075_{-0.375}^{+0.455} \times 10^{-6}$ , value that is compatible with the values obtained from the simulations of the evolution of the string network from  $z = 100$  to present [24], as well as with other existing studies of the expected large-scale CMB anisotropy [21], [25,26].

## Acknowledgements

This work was partially supported by M.C.T. grant 3005GR. The COBE-*DMR* data sets, developed by NASA Goddard Space Flight Center under the guidance of the COBE Science Working group, were provided by the NSSDC.

## References

- [1] A.H. Guth, Phys. Rev. **D 23** (1981) 347
- [2] A. Linde, Phys. Lett **B 108** (1982) 389
- [3] A. Liddle and D. Lyth, Phys. Rep. **231** (1993) 1
- [4] A. Vilenkin, Phys. Rep. **121** (1985) 263.
- [5] A. Vilenkin and E.P.S. Shellard *Cosmic Strings and Other Topological Defects* (Cambridge University Press, 1994)
- [6] D. Coulson, P. Ferreira, P. Graham, and N. Turok Nature **368** (1994) 27
- [7] L. Kofman, A. Linde and A.A Starobinsky Phys. Rev. Lett. **76** (1996) 1011



- [8] A. Albrecht, D. Coulson, P. Ferreira and J. Magueijo Phys. Rev. Lett **76** (1996) 1413
- [9] J. Magueijo, A. Albrecht, D. Coulson and P. Ferreira Phys. Rev. Lett. **76** (1996) 2617
- [10] P. Ferreira and J. Magueijo Phys. Rev. **D 55** (1997) 3358
- [11] R. Crittenden and N. Turok Phys. Rev. Lett. **75** (1995) 2642
- [12] M. Kendall, A. Stuart and J.K. Ord *Kendall's Advanced Theory of Statistics* (Oxford University Press, New York, 1987)
- [13] H.A. Feldman, N. Kaiser, J.A. Peacock Ap. J. **426** 23.
- [14] A.J. Stirling and J.A. Peacock MNRAS **283L** (1996) 99
- [15] C.K. Chui, *An Introduction to Wavelets* (Academic Press, 1992)
- [16] W.H. Press, B.P. Flannery, S.A. Teukolsky, W.T. Vetterling *Numerical Recipes* (Cambridge University Press, 1992)
- [17] D. Bennet and F. Bouchet, Phys. Rev. Lett. **60** (1988) 257
- [18] B. Allen and E.P.S. Shellard Phys. Rev. Lett. **64** (1990) 119
- [19] N. Kaiser and A. Stebbins Nature **310** (1984) 391
- [20] R. Moessner, L. Privolaropoulos, and R. Branderberger, Ap. J. **425** (1994) 365
- [21] L. Perivolaropoulos, Phys Lett. **B298** (1993) 305
- [22] J.R. Bond and G. Efstathiou, MNRAS **226** (1987) 655
- [23] Y. Fujiwara and J. Soda, Prog. Theor. Phys. **95** (1996) 1059
- [24] B. Allen, R.R. Caldwell, E.P.S. Shellard, A. Stebbins and S. Veeraraghavan Phys. Rev. Lett. **77** (1996) 3061
- [25] D. Bennet, A. Stebbins, and F. Bouchet, Ap.J.Lett **399** (1992) L5
- [26] T. Hara, P. Mahonen, and S.Miyoshi, Ap.J **414** (1993) 412

## Figure Captions

### Figure 1.

Number of spots as a function of threshold for an averaged map obtained for: a)  $a_{lm}$  with gaussian random phases, b) the wavelet transformed of the gaussian maps, c)  $a_{lm}$  with non-gaussian random phases (see text), d) the wavelet transformed of non-gaussian maps. The gaussian fits for each case are also shown.

### Figure 2.

The 2-point function of the power fluctuations in the wavelet space: with the continuous line is the theoretical prediction if the underlying distribution is gaussian and  $Q_{rms-PS} = 18\mu\text{K}$ . The error bars are based on Monte-Carlo simulations in the cosmic string model with  $M = 10$  and the same normalization.

### Figure 3.

$I(\chi^2)$  for the models with  $Q_{rms-PS} = 18\mu\text{K}$  and  $M=4, 6, 9$  and  $10$  (from bottom to top) and the same probability in the gaussian case (the upper curve).

### Figure 4.

The confidence regions for  $Q_{rms-PS}$  and  $M$  at 68% CL for Gaussian statistics.

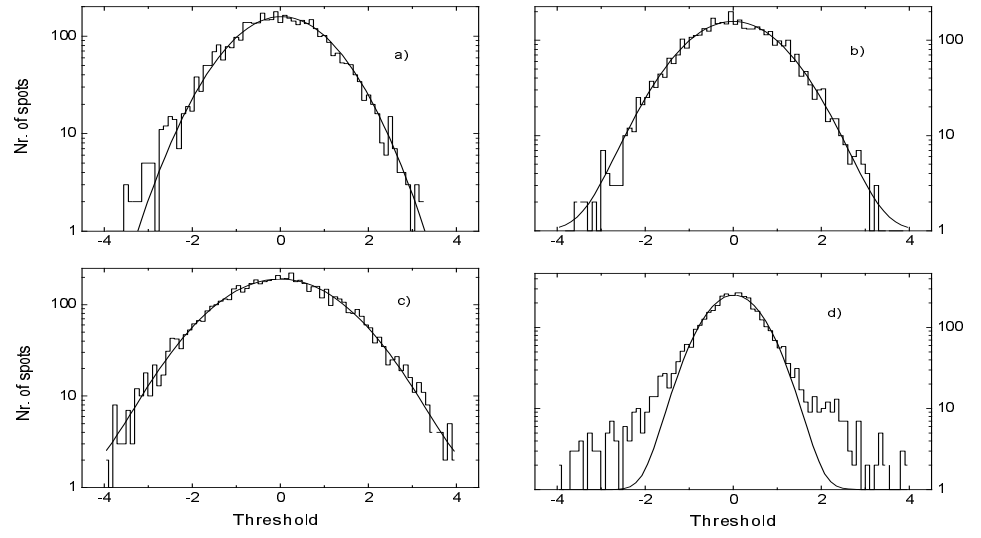


Figure 1:

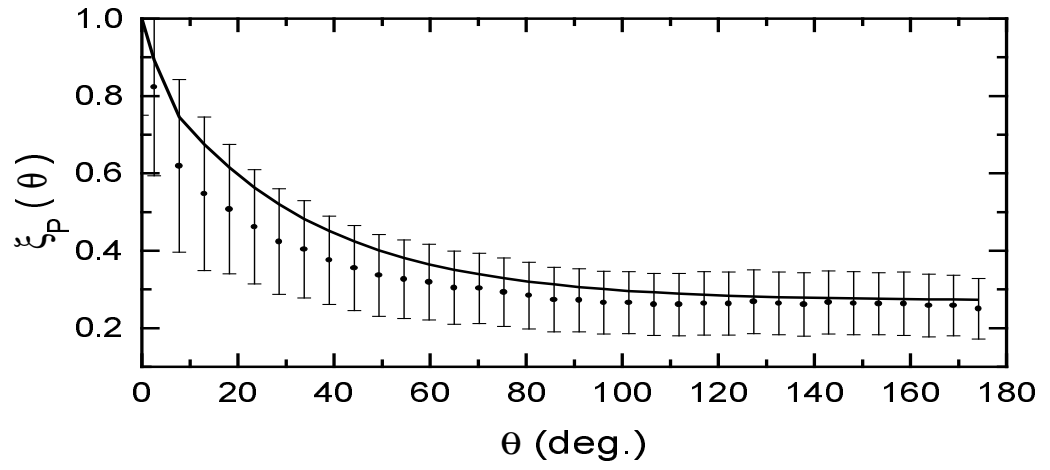


Figure 2:

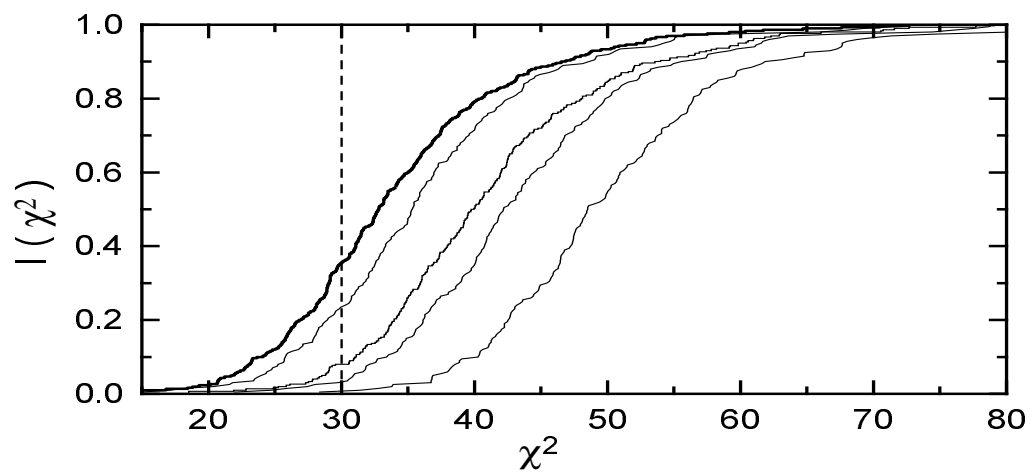


Figure 3:

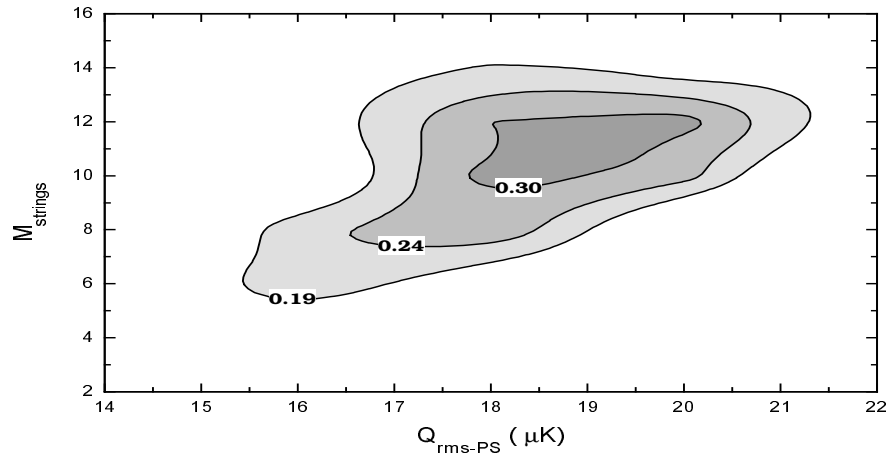


Figure 4: